Current Applied Physics 13 (2013) 26–30

Contents lists available at SciVerse ScienceDirect

Current Applied Physics

journal homepage: www.elsevier.com/locate/cap

Electrical transport studies of MBE grown InGaN/Si isotype heterojunctions

Mahesh Kumar [a,b,*], Basanta Roul [a,b], Mohana K. Rajpalke [a], Thirumaleshwara N. Bhat [a], A.T. Kalghatgi [b], S.B. Krupanidhi [a,**]

[a] Materials Research Centre, Indian Institute of Science, Bangalore 560012, India
[b] Central Research Laboratory, Bharat Electronics, Bangalore 560013, India

ARTICLE INFO

Article history:
Received 18 May 2012
Received in revised form
7 June 2012
Accepted 8 June 2012
Available online 26 June 2012

Keywords:
Nitrides
MBE
Heterojunctions

ABSTRACT

The temperature dependent electrical transport behavior of *n*–*n* InGaN/Si heterostructures grown by plasma-assisted MBE was studied. Structural characteristics of the as-grown InGaN epilayers were evaluated high resolution X-ray diffraction and composition of InGaN was estimated from photoluminescence spectra using standard Vegard's law. Current density–voltage plots (*J*–*V*–*T*) revealed that the ideality factor (η) and Schottky barrier height (SBH) (Φ_b) are temperature dependent and the incorrect values of the Richardson's constant (A^{**}) produced, suggests an inhomogeneous barrier at the heterostructure interface. The higher value of the ideality factor compared to the ideal value and its temperature dependence suggest that the current transport is mainly dominated by thermionic field emission.

1. Introduction

In the past decade, InGaN alloys have been attracted a lot of attention because of the band gap of this material system ranges from the infrared to the ultraviolet region (0.7–6.2 eV). This direct and wide band gap range makes the InGaN material system useful for photovoltaic applications, blue- and green-light emitting diodes, ultraviolet detectors and field-effect transistors [1–3]. InGaN has been grown either on Si or Al_2O_3 using AlN, GaN and InN layers [4–6]. However, the band alignment of InGaN and Si can be exploited for the fabrication of tandem InGaN/Si heterojunction solar cells that may have power conversion efficiency higher than 30% [7]. Ager III et al. (Ref. [8]) reported, an unpinned *n*-InGaN/*p*-Si anisotype junction should have little band bending at the interface and efficient electron–hole recombination and ohmic behavior is predicted. In the case of an ideal *n*-InGaN/*n*-Si isotype junction, due to the large electron affinity of the InGaN, there is depletion on the Si side of the junction and rectifying behavior would be predicted. Schematic band diagram of *n*-$In_{0.2}Ga_{0.8}N$/*n*-Si and *n*-$In_{0.2}Ga_{0.8}N$/*p*-Si junctions are shown in Fig. 1. In this work, we have investigated the temperature dependent electrical transport properties of *n*–*n* InGaN/Si heterojunctions.

2. Experimental details

The growth system used in this study was a plasma-assisted MBE system (OMICRON). The plasma source used in this work was an Oxford Scientific (RF OSPrey) RF plasma source with a frequency of 13.56 MHz. RF energy is used to create a nitrogen plasma from which neutral species are allowed to effuse out into the vacuum chamber [9]. The base pressure in the system was below 1×10^{-10} mbar. The *n*-type 2-inch Si (1 1 1) substrates were ultrasonically degreased and boiled in trichloroethylene, acetone and methanol at 70 °C for 5 min, respectively, followed by dipping in 5% HF for 30 s to remove the surface oxide. The substrates were thermally cleaned at 900 °C for 6 h in ultra-high vacuum (9×10^{-10} mbar). The substrates were exposed to the Gallium (Ga) and Indium (In) molecular beams at 400 °C for 60 s (~2 monolayers) to avoid the formation of amorphous silicon nitride [10]. Further, the substrate temperature was increased to 550 °C and 300 nm thick InGaN epilayers were grown on Si. The Ga and In effusion cells were kept 880 °C and 780 °C and corresponding beam equivalent pressures (BEP) were maintained 1.2×10^{-7} and 2.1×10^{-7} mbar, respectively. The nitrogen flow rate and RF-plasma power were kept 1 SCCM and 350 W, respectively. The structural evaluations of InGaN layers were carried out by high resolution X-ray diffraction (HRXRD). The Photoluminescence (PL) spectra were recorded at room temperature using a He–Cd laser of 325 nm excitation wavelength with a maximum input power of 30 mW. InGaN/Si interface was examined by using cross-section transmission electron microscopy (TEM). The Hall measurements were

* Corresponding author. Materials Research Centre, Indian Institute of Science, Bangalore 560012, India. Tel.: +91 8022932943.
** Corresponding author.
E-mail addresses: mkchahar@mrc.iisc.ernet.in (M. Kumar), sbk@mrc.iisc.ernet.in (S.B. Krupanidhi).

1567-1739/$ – see front matter © 2012 Elsevier B.V. All rights reserved.
http://dx.doi.org/10.1016/j.cap.2012.06.015

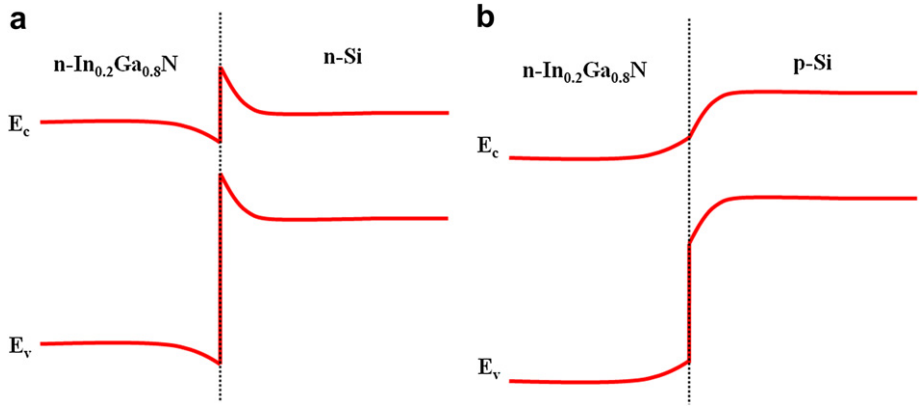

Fig. 1. Schematic band diagram of (a) n-$In_{0.2}Ga_{0.8}N$/n-Si and (b) n-$In_{0.2}Ga_{0.8}N$/p-Si junctions.

conducted under 0.55 T magnetic fields. Samples of 5×5 mm^2 size were cut from the wafers and Indium metal droplets served as contacts in the four corners to obtain electrical contacts in the van der Pauw geometry. The circular contacts of diameter 400 μm were made on InGaN as well as on Si surface by thermally depositing Al (thickness ~ 300 nm) metal and followed by thermal annealing at 200 °C for 30 min. The adequate Ohmic nature of the contacts to InGaN and Si was verified. The device transport characteristics were studied at various temperatures using the probe station attached with the KEITHLEY-236 source measure unit.

3. Result and discussions

Structural characteristics of the as-grown InGaN layers were evaluated by HRXRD and shown in Fig. 2(a). A strong (0 0 0 2) and a weak (0 0 0 4) InGaN diffracted peaks were observed at $2\theta = 33.94°$ and at $2\theta = 71.66°$, respectively. The HRXRD results indicating the InGaN layers to be highly oriented along the [0 0 0 1] direction of the wurtzite structures of InGaN. Fig. 2(b) shows 1 μ × 1 μ AFM image of 300 nm thick InGaN layers grown on Si (1 1 1) and the root mean square (RMS) roughness of the InGaN layers is ~1.43 nm. InGaN/Si interface was examined by using cross-section TEM. Fig. 2(c) represents typical high resolution TEM (HRTEM) and observation shows a sharp interface. A PL spectrum of InGaN film recorded at room temperature is shown in Fig. 2(d), which contains a strong near band-edge emission (NBE) around ~2.46 eV. The composition of $In_{0.2}Ga_{0.8}N$ was calculated by using Vegard's law [11].

The transport measurements on the Si substrate and InGaN layers were done using a Hall mobility setup. Hall measurements revealed n-type conductivity, with donor concentrations $\sim 7.2 \pm 1 \times 10^{18}$ cm^{-3} at room temperature. The contact resistance of Al/$In_{0.2}Ga_{0.8}N$ was found 2.8×10^{-3} Ω cm^2. The current density–voltage–temperature (J–V–T) characterization of the n–n InGaN/Si heterojunctions was performed in order to determine the significant parameters ruling the current transport across the junction, namely, the ideality factor (η) and the SBH (Φ_b). Fig. 3 shows forward J–V characteristics of the InGaN/Si heterojunctions, which were acquired in the temperature range of 200–450 K. At fixed bias the forward current increases with increasing temperature, which indicates that the current may be induced by the thermionic emission (TE). From TE theory [12,13]

$$J = J_s\{\exp(qV/\eta kT) - 1\}, \quad (1)$$

where J_s is the saturation current expressed by

$$J_s = A^{**}T^2\exp(-q\Phi_b/kT). \quad (2)$$

Here, A^{**} is the Richardson's constant (112 A cm^{-2} K^{-2} for n-type Si) [14], k is the Boltzmann's constant, q is the electron charge and T is the measurement temperature. The values of SBH (Φ_b) and the ideality factor (η) for the junction were calculated as a function of measuring temperature by fitting a line in the linear region of the forward J–V curves using the TE equation. The fitting curve of the J–V characteristics in the TE regime is also shown in Fig. 3. The value of Φ_b and η obtained from J–V–T measurements based on TE model are given in Table 1. We found that the experimental values of Φ_b decreased with a decrease in temperature and the experimental values of η increased with a decrease in temperature. Thus, these investigations on temperature dependence of Φ_b indicate that the SBH is inhomogeneous in nature and the inhomogeneous SBH may be due to various types of defects that could be present at the InGaN/Si interface.

The values of the saturation current density (J_s) were obtained at each temperature from the J–V data and Fig. 4 shows the conventional Richardson's plot of ln (J_s/T^2) versus $1/kT$. The Richardson's constant and Schottky barrier height were calculated 4.8×10^{-4} A cm^{-2} K^{-2} and 0.19 eV, respectively. The value of Richardson constant and barrier height obtained from the conventional Richardson plot is much lower than the theoretical values, suggesting the formation of an inhomogeneous SBH at the interface. In order to take into account of temperature dependent ideality factor and SBH, the modified Richardson's plot [15] of ln (J_s/T^2) versus $1/\eta kT$ is shown in Fig. 4. From the linear fit of the modified plot, the Richardson's constant and the barrier height were calculated to be 118 A cm^{-2} K^{-2} and 0.63 eV, respectively. The value of Richardson constant obtained from the modified Richardson plot was found to be closer to the theoretical value (112 A cm^{-2} K^{-2} for n-type Si) [14].

For n-type Si substrate used in this study, the carrier concentration (N_d) values obtained from Van der Pauw–Hall measurements in the temperature range of 200–450 K are given in Fig. 5. The effective density of states (N_c) for n-type Si, that is, $N_c = 2(2\pi m^* kT/h^2)^{3/2}$, the N_c values calculated in the temperature range of 200–450 K are also given in Fig. 5. m^* ($m^* = 0.259\, m_0$ for n-type Si [16], m_0 is the mass of electron at rest) is the electron effective mass and h is Planck's constant. The N_c of the n-type Si decreased remarkably with a decrease in temperature and N_c at 450 K is approximately four times greater than that at 200 K. When the concentration of electrons in the conduction band exceeds N_c, the Fermi energy lies within the conduction band. The type of semiconductor is called degenerate n-type semiconductor. In the present case, it can see that N_c is close to N_d at 200 K, leading to a remarkable reduction in the energy difference (V_n) between the conduction band minimum (E_C) and Fermi level (E_F) in n-type Si. V_n was assumed to be $V_n = kT/q \ln(N_c/N_d)$ [17] in this study and shown

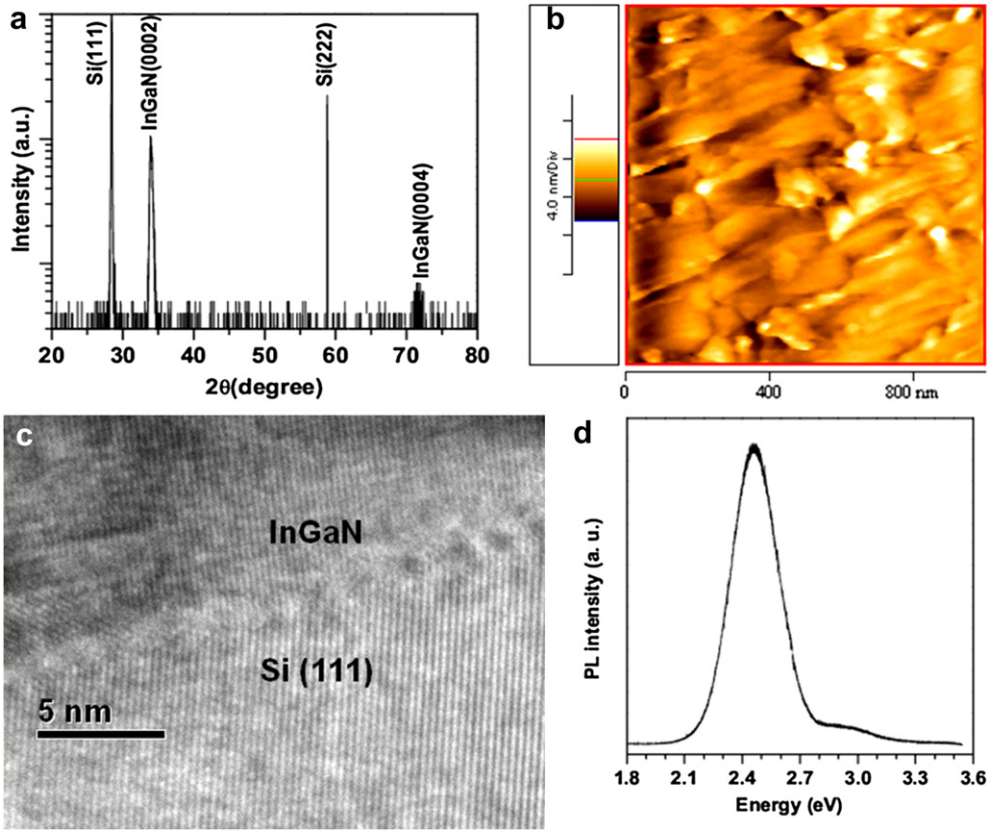

Fig. 2. (a) HRXRD $2\theta - \omega$ scan and (b) 1 μ × 1 μ AFM image of InGaN epilayers. (c) Cross-section HRTEM of InGaN/Si interface and (d) room temperature PL spectrum of InGaN epilayers grown on Si (1 1 1).

in Fig. 5. From the figure, it can be seen that V_n decreased with decreasing in temperature. The decrease in V_n might cause a tunneling effect at the InGaN/Si interface, resulting in the increase in η. The observations strongly support the existence of current conduction mechanisms other than the TE process, such as tunneling [18]. In this study, a TFE model involving the occurrence of near degeneration is proposed to account for the larger η observed at low temperature.

If the current transport obeys the TFE theory, the J–V characteristic of a Schottky diode can be given by [19,20]

$$J = J_0 \exp(qV/E_0), \tag{3}$$

$$E_0 = E_{00}\coth(E_{00}/kT) = \eta kT, \tag{4}$$

$$J_0 = \frac{A^* T\sqrt{\pi E_{00}\left(\Phi_{btfe} - qV - V_n\right)}}{k\cosh\left(\frac{E_{00}}{kT}\right)}\exp\left[-\frac{V_n}{kT} - \frac{\left(\Phi_{btfe} - V_n\right)}{E_0}\right] \tag{5}$$

Here, E_{00} is the tunneling parameter, is related to the tunnel transmission probability and is given by Ref. [21]

$$E_{00} = \frac{h}{4\pi}\left(\frac{N_d}{m^*\varepsilon_s}\right)^{1/2}. \tag{6}$$

where m^* is the effective mass of the electron and ε_s is the dielectric constant of Si. Taking the values of $m^* = 0.259\ m_0$ [16] and

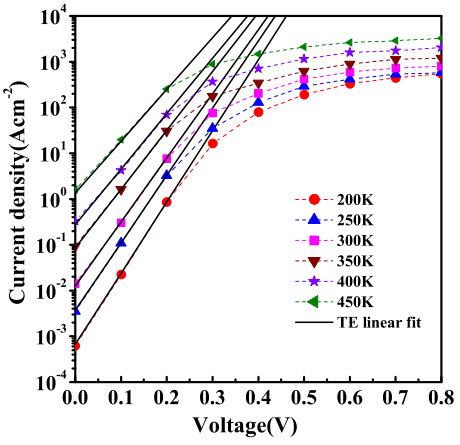

Fig. 3. The forward J–V characteristics of InGaN/Si Schottky diode as a function temperature and the TE fitting to the J–V characteristics.

Table 1
The values of barrier height and ideality factor of the InGaN/Si heterojunctions in the temperature range of 200–450 K obtained by using TE and TFE models.

Temp. (K)	TE		TFE	
	η	Φ_b	η	Φ_b
200	1.62	0.39	1.59	0.70
250	1.37	0.46	1.38	0.715
300	1.20	0.525	1.25	0.74
350	1.12	0.57	1.18	0.76
400	1.03	0.61	1.12	0.77
450	0.99	0.64	1.06	0.78

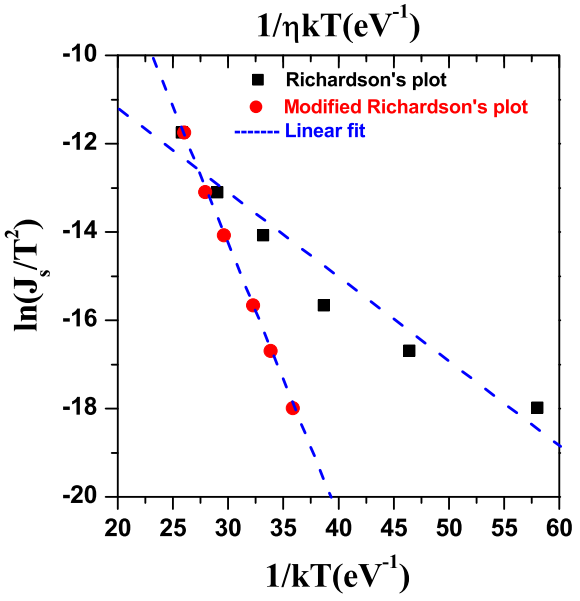

Fig. 4. The conventional Richardson's plot of ln (J_s/T^2) vs $1/kT$ and the modified Richardson's plot of ln (J_s/T^2) vs $1/kT$.

$\varepsilon_s = 11.8\ \varepsilon_0$ [22], calculated as well as experimental values of E_{00}/kT and E_0/kT are given in Table 2. The TFE model has been applied to the experimental J–V characteristics in order to calculate Φ_{btfe} and η. The values of Φ_{btfe} and η at different temperatures were obtained from the linear region of the forward J–V characteristics by fitting Eq. (3) are given in Table 1. The fitting curve using the TFE model is shown in Fig. 6. From the Table 1 it can be seen, the ideality factors obtained from the TE and TFE models are almost the same but there is a difference in the SBHs obtained from TE and TFE models. We found that SBH obtained from TFE model for the InGaN/Si Schottky diode is less sensitive to measurement temperature than that obtained from TE model. We also found that Φ_{btfe} determined from J–V measurements based on TFE model is higher than Φ_b determined from J–V measurements based on TE model. The calculated value of E_{00}/kT at room temperature was found to be 0.581 but the experimental value for the E_{00}/kT was found to be 0.896. Tung et al. [23] reported that the TFE becomes import when $E_{00}/kT \approx 1$, while TE is important when $E_{00}/kT << 1$. Since, in the present case

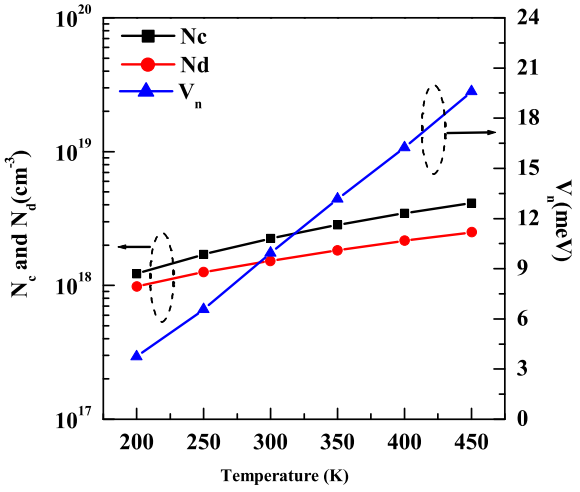

Fig. 5. The variation of N_c, N_d and V_n as a function of the temperature for n-type Si.

Table 2
Calculated and experimental electrical parameters of the InGaN/Si heterojunctions in the temperature range of 200–450 K obtained by using TFE model.

Temp. (K)	E_{00}/kT		$\eta = E_0/kT$	
	Calculated values	Experimental values	Calculated values	Experimental values
200	0.646	1.413	1.14	1.59
250	0.593	1.115	1.12	1.38
300	0.581	0.896	1.11	1.25
350	0.551	0.761	1.10	1.19
400	0.542	0.587	1.10	1.11
450	0.544	0.439	1.10	1.06

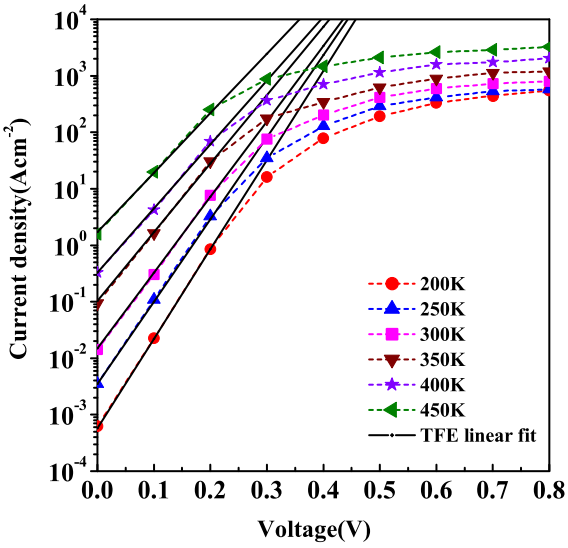

Fig. 6. The forward J–V characteristics of InGaN/Si Schottky diode as a function temperature and the TFE fitting to the J–V characteristics.

$E_{00}/kT \approx 1$, it suggests that TFE can be considered to be a more reasonable model for the analysis of the electronic transport in InGaN/Si heterostructure.

4. Conclusion

The InGaN/Si heterostructures were fabricated by plasma-assisted MBE. Structural characteristics of the as-grown InGaN epilayers were evaluated HRXRD and from the PL spectra, the composition of $In_xGa_{1-x}N$ was calculated to be $\sim x = 0.2$. The temperature dependence of the electrical properties of the n–n $In_{0.2}Ga_{0.8}N$ heterostructures based Schottky diode has been investigated. It is found that the barrier height and ideality factor of the Schottky diode are strongly temperature dependent. It is found that $E_{00}/kT \approx 1$ for InGaN/Si heterostructure, which suggests that TFE can be considered to be a more suitable model for the analysis of the electronic transport in this heterojunction.

References

[1] C.J. Neufeld, N.G. Toledo, S.C. Cruz, M. Iza, S.P. DenBaars, U.K. Mishra, Appl. Phys. Lett. 93 (2008) 143502.
[2] O. Jani, I. Ferguson, C. Honsberg, S. Kurtz, Appl. Phys. Lett. 91 (2007) 132117.
[3] S.C. Jain, M. Willander, J. Narayan, R. Van Overstraeten, J. Appl. Phys. 87 (2000) 965.
[4] A. Krost, A. Dadgar, Mater. Sci. Eng. B 93 (2002) 77.
[5] C.A. Tran, R.F. Karlicek Jr., M. Schurman, A. Osinsky, V. Merai, Y. Li, I. Eliashevich, M.G. Brown, J. Nering, I. Ferguson, R. Stall, J. Cryst. Growth 195 (1998) 397.
[6] D.N. Nath, E. Gur, S.A. Ringel, S. Rajan, Appl. Phys. Lett. 97 (2010) 071903.

[7] J.W. Ager III, L.A. Reichertz, D. Yamaguchi, L. Hsu, R. E.Jones, K.M. Yu, W. Walukiewicz, W.J. . Schaff, in: Proceedings of 22nd European Photovoltaic Solar Energy Conference and Exhibition, Milan, Italy (2007), pp. 215–218.
[8] J.W. Ager III, L.A. Reichertz, Y. Cui, Y.E. Romanyuk, D. Kreier, S.R. Leone, K.M. Yu, W.J. Schaff, W. Walukiewicz, Phys. Status Solidi C 6 (2009) S413.
[9] M.A. Herman, H. Sitter, Molecular Beam Epitaxy Fundamentals and Current Status, vol. 7, Springer Series in Materials Science, 1996.
[10] X.Y. Liu, H.F. Li, A. Uddin, T.G. Andersson, J. Cryst. Growth 300 (2007) 114.
[11] M. Kumar, B. Roul, T.N. Bhat, M.K. Rajpalke, A.T. Kalghatgi, S.B. Krupanidhi, Jpn. J. Appl. Phys. 51 (2012) 020203.
[12] L. Wang, M.I. Nathan, T. Lim, M.A. Khan, Q. Chen, Appl. Phys. Lett. 68 (1996) 1267.
[13] Hadis Morkoç, Handbook of Nitride Semiconductors and Devices, Wiley-VCH, New York, 2008.
[14] C. Hayzelden, J.L. Batstone, J. Appl. Phys. 73 (1993) 8279.
[15] R. Hackam, P. Harrop, IEEE Trans. Electron Devices 19 (1972) 1231.
[16] D.M. Riffe, J. Opt. Soc. Am. B 19 (2002) 1092.
[17] Y.J. Lin, Appl. Phys. Lett. 86 (2005) 122109.
[18] H. Kim, J. Ryou, R.D. Dupuis, S.N. Lee, Y. Park, J. Weon, T.Y. Seong, Appl. Phys. Lett. 93 (2008) 192106.
[19] Y.J. Lin, S.S. Chang, H.C. Chang, Y.C. Liu, J. Phys. D: Appl. Phys. 42 (2009) 075308.
[20] L. Stafford, L.F. Voss, S.J. Pearton, J.J. Chen, F. Ren, Appl. Phys. Lett. 89 (2006) 132110.
[21] K. Cinar, N. Yildirim, C. Coskun, A. Turut, J. Appl. Phys. 106 (2009) 073717.
[22] B. Streetman, S. Banerjee, Solid State Electronic Devices, sixth ed. (2005).
[23] R.T. Tung, Mater. Sci. Eng. R 35 (2001) 1.